

Magnetic anisotropy of the nickel-doped spin-Peierls cuprate CuGeO_3

P. E. Anderson, J. Z. Liu, and R. N. Shelton

Department of Physics, University of California, Davis, California 95616

(Received 23 December 1997)

The magnetization of single crystals in the system $(\text{Cu}_{1-x}\text{Ni}_x)\text{GeO}_3$ has been measured for compositions in the range $0.000 \leq x \leq 0.055$. As the value of x is increased, the spin-Peierls transition temperature (T_{sp}) decreases from 14.5 K ($x=0.000$) to less than 10 K for $x>0.030$. For $x>0.021$, antiferromagnetic order is observed, with the Néel temperature (T_N) below 5 K. Significantly, the easy axis in the ordered state for Ni doping is the a axis as opposed to the c axis, as observed for $(\text{Cu}_{1-x}\text{M}_x)\text{GeO}_3$ ($M=\text{Zn}, \text{Co}, \text{Mn}$). The angular dependence of the magnetization was investigated, along with the spin-flop behavior, and values of the anisotropy energy are reported as a function of doping level and temperature assuming uniaxial symmetry. [S0163-1829(98)11117-7]

I. INTRODUCTION

The ternary oxide CuGeO_3 has received considerable attention in the past few years because it was the first known inorganic spin-Peierls compound.¹ The crystal structure of CuGeO_3 was determined first by Völlenkne *et al.*,² and recently reexamined by Hidaka *et al.*³ The compound is composed of chains of Cu^{+2} spin-1/2 ions along the c axis, leading to quasi-one-dimensional magnetic interactions. The trademark feature of the spin-Peierls transition is a drop in the magnetic susceptibility caused by the dimerization of the chain in order to form spin-0 dimers.

Unlike the organic compounds studied previously, the spin-Peierls transition in CuGeO_3 can be studied through doping on either the Cu site or the Ge site. Numerous reports on the effects of doping have appeared in the literature, including single-crystal experimental data and theoretical models. The copper-site substitutions investigated include Zn,⁴ Mg,⁵ Ni,⁶ Co,⁷ and Mn.^{6,8}

Since the ions mentioned above have spin-0, 0, 1, 3/2, and 5/2, respectively, these substitutions are interesting because they introduce nonzero magnetic moments in the ordered spin-Peierls state. However, the spin of the in-chain dopant appears to play almost no role in the destruction of spin-Peierls order, for regardless of the dopant it is found that replacing a relatively small fraction of the Cu^{+2} ions suppresses T_{sp} rapidly. In the case of cobalt doping for example, $T_{\text{sp}}=11.3$ K for $x=0.023$.⁷

As the doping level is increased, magnetization data show coexistence of spin-Peierls order and long-range antiferromagnetic order. As even more impurity moments are added, the regions of their influence begin to overlap, and the system orders antiferromagnetically. The published phase diagrams which rely on magnetization data^{5,9,7} indicate that T_{sp} is suppressed rapidly for the same narrow range of compositions in which T_N is increasing rapidly. A neutron-diffraction study¹⁰ of Zn doping, on the other hand, indicates that the coexistence occurs for a wider range of compositions, at least in the Zn-doped system.

The spin of the dopant is expected to play a more significant role in the formation of the Néel state, and in particular, the magnitude of T_N , and its dependence on doping level.

However, there is another aspect of the Néel state which has not been reported, as far as these authors know, and that is the change in easy-axis direction as a function of dopant. The easy axis for the antiferromagnetic ordered state in $(\text{Cu}_{1-x}\text{M}_x)\text{GeO}_3$ is the c axis for $M=\text{Zn}, \text{Co}$, and Mn , and the a axis for $M=\text{Ni}$. Since the Néel state forms with only a few percent of impurity spins, it is clear that the antiferromagnetically ordered state must include a large fraction of the remaining Cu ions. As a result, the magnetic anisotropy should depend in part on the local environment of the Cu ions, which does not change for different dopants. Therefore, our experimental observation that the easy axis is different when Ni impurities are introduced into the system is noteworthy, reflecting the fundamental nature of the magnetic spin interactions in these materials.

To explore this strange result, we have studied the magnetic anisotropy of $(\text{Cu}_{1-x}\text{Ni}_x)\text{GeO}_3$ through detailed measurements of the spin-flop transition and the angular dependence of the magnetization. In addition to the phase diagram, we report values of the anisotropy energy (K) as a function of doping level and scaled temperature (T_N-T).

II. SAMPLE PREPARATION AND CHARACTERIZATION

The $(\text{Cu}_{1-x}\text{Ni}_x)\text{GeO}_3$ single crystals were grown using the self-flux method, with a charge of 10 g. The constituent oxides: CuO, NiO, and GeO_2 were mixed and well ground using an agate mortar and pestle. An additional 10% by mass of CuO and NiO was added to act as the flux. The single crystals were grown in a platinum crucible, by slow cooling from 1170 ± 10 °C. Individual crystals were separated mechanically from the melt.

A commercial wavelength dispersive electron microprobe¹¹ was used to determine the actual composition of the $(\text{Cu}_{1-x}\text{Ni}_x)\text{GeO}_3$ crystals. Each crystal was sampled with 2–3 lines of 5–8 points. The data are shown in Fig. 1. Unlike Co-doped crystals grown under similar conditions,⁷ the actual composition of the Ni-doped crystals is consistently higher than the nominal composition.

III. EXPERIMENT

The magnetization data as a function of temperature and field were measured using a commercial superconducting

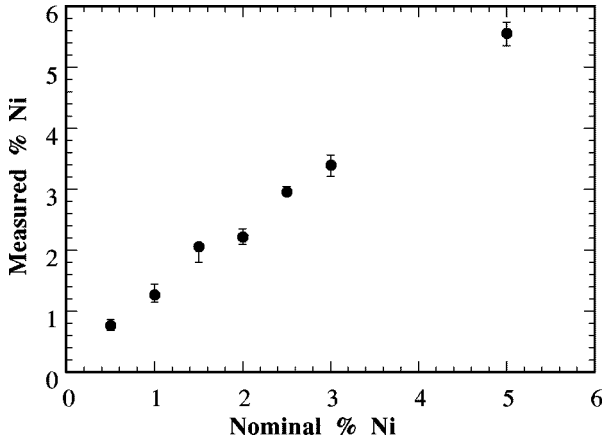


FIG. 1. The nickel doping level as measured by electron microprobe versus the nominal doping level for $(\text{Cu}_{1-x}\text{Ni}_x)\text{GeO}_3$ single crystals. The error bars indicate the range of measured values.

quantum interference device magnetometer.¹² All samples were zero-field cooled to 1.8 K and measured in a magnetic field of 0.1 T. There is no evidence of hysteresis. For each composition, the magnetization of a single crystal was measured with the applied field directed along each of the three principal axes, in turn. For the data reported here, the sample masses range from 20 to 80 mg. Measurements of different crystals from the same melt were found to be consistent with each other. The susceptibilities of $(\text{Cu}_{1-x}\text{Ni}_x)\text{GeO}_3$ as a function of temperature for various values of x are plotted in Fig. 2.

Using a custom probe, the angular dependence of the susceptibility was studied below the Néel temperature, with measurements approximately every 10° between the principal axes at 1.8 K with $H=0.1$ and 2 T. These data are shown in Fig. 3. The mass of the $(\text{Cu}_{0.944}\text{Ni}_{0.056})\text{GeO}_3$ single crystal was 31.3 mg, while the mass of the $(\text{Cu}_{0.97}\text{Co}_{0.03})\text{GeO}_3$ single crystal was 9.8 mg.

The magnetic-field dependence of these samples in the ordered antiferromagnetic state was studied in detail. Again, the samples were zero-field cooled. Magnetization curves from 0.0 to 5.5 T were measured every 0.25 K, from 1.8 K to T_N , which varies as a function of doping level. Near the spin-flop transition, the magnetization was measured every 0.005 T in order to determine the critical field H_c . The molar susceptibility as a function of applied field, with H parallel to each of the principal axis directions, is shown in Fig. 4 for a 5.6% Ni crystal at $T=2$ K. The spin-flop critical field, as determined from the data, is indicated in the plot. These data are representative of the data for other Ni compositions which exhibit a low-temperature Néel phase; namely, for $x \geq 0.021$.

IV. ANALYSIS AND DISCUSSION

The magnetic phase diagram as determined by the susceptibility measurements is shown in Fig. 5. The spin-Peierls and Néel phases are labeled. Both the spin-Peierls temperature and the Néel temperature were determined by the intersection of linear fits to the data on either side of the transition. As the plot shows, the system orders antiferromagnetically for $x \geq 0.021$, and the spin-Peierls tran-

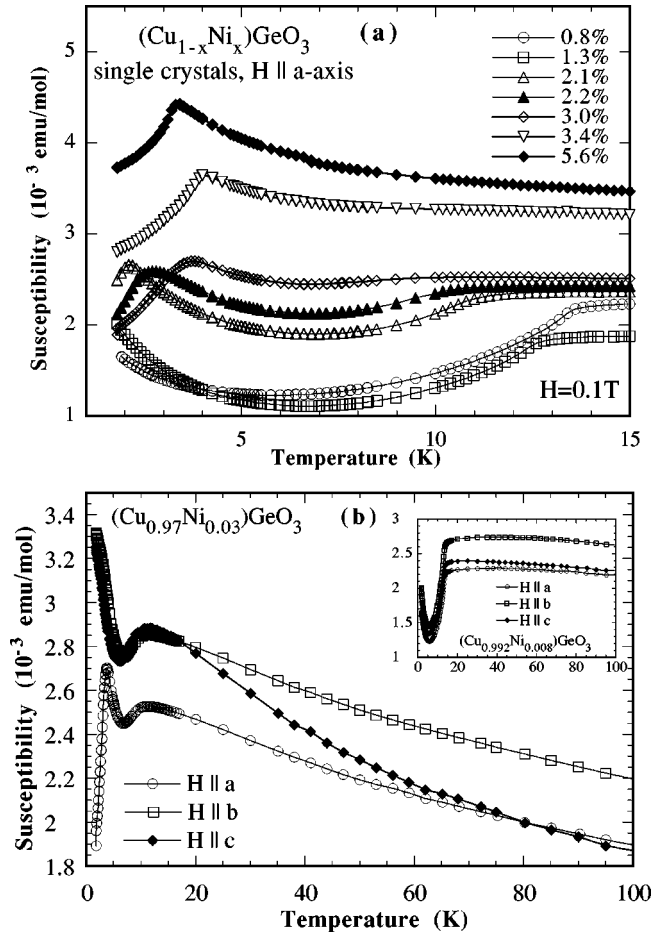


FIG. 2. The a -axis magnetic susceptibility (a) of $(\text{Cu}_{1-x}\text{Ni}_x)\text{GeO}_3$ single crystals, where $0.000 < x < 0.056$, showing the antiferromagnetic ordering peak, and the spin-Peierls transition. All compositions were measured with $H=0.1$ T. A comparison (b) of the magnetic susceptibility with the applied field directed along each of the principal axes directions for $x=0.008$ (inset) and $x=0.030$.

sition is apparent for $x \leq 0.030$, although the susceptibility data suggest that the spin-Peierls phase exists for higher concentrations. Either way, our data show an overlap region in which spin-Peierls and antiferromagnetic order are both observed, with $T_{sp} > T_N$.

Our phase diagram for Ni-doped CuGeO_3 agrees qualitatively with the results of other authors,^{6,13,9} although there are small differences. The values of T_{sp} as a function of the Ni-doping level reported by Weiden⁹ are consistently lower than our reported values. In addition, we observe antiferromagnetic order at a lower Ni composition; $T_N=2.0$ K for $x=0.021$.

Of the compositions we measured, the Néel temperature reaches a peak value of 4.0 K for $x=0.034$, and decreases for higher compositions. This feature is present in other published phase diagrams, and is due to frustration. Once the average nickel spacing is comparable to the length scale of the induced magnetic moment surrounding each nickel, the system orders antiferromagnetically. Adding more nickel results in competing exchange interactions, and the Néel temperature decreases.

The anisotropy of the susceptibility for the system has

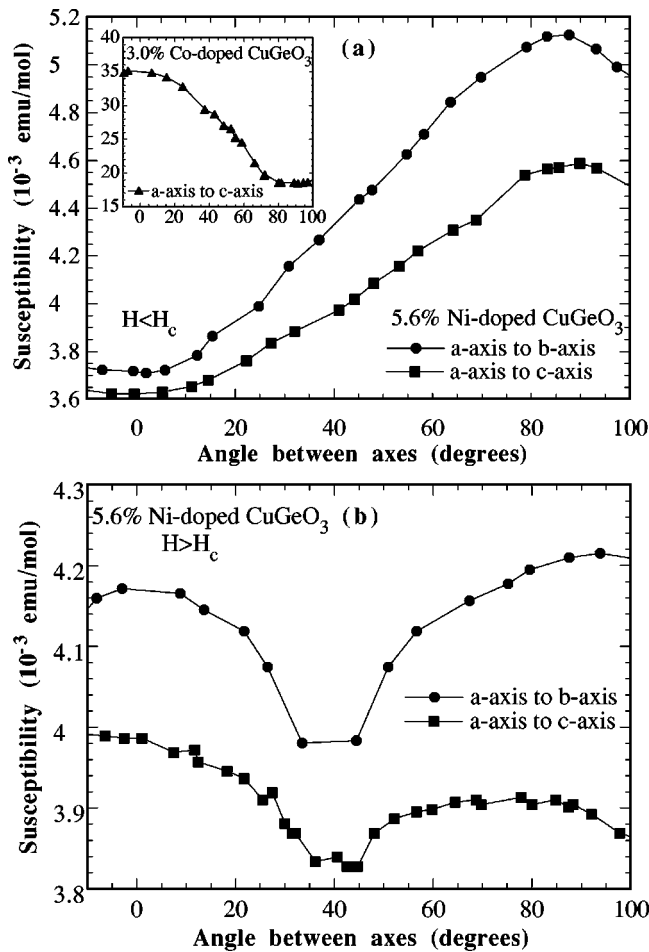


FIG. 3. The molar susceptibility as a function of angle between the principal axes for a 5.6% Ni-doped CuGeO_3 single crystal. The applied field was 0.1 T in (a) and 2 T in (b), and the measurements were made at 1.8 K. The inset plot in (a) is the susceptibility as a function of angle for a 3% Co-doped CuGeO_3 single crystal.

two notable qualitative features, which are exemplified in Fig. 2(b). First, whether or not this compound is doped, we observe temperature-independent magnetic anisotropy. For example, the susceptibility with the field directed along the b axis is greater for all compositions, but has the same shape as the susceptibility measured along at least one of the other axes. This temperature-independent anisotropy is evident in the pure CuGeO_3 data published by Hase.¹

Second, in the temperature range $T_{sp} < T < 100$ K, the c -axis Ni-doped data have a more negative slope than the other two directions, decreasing from near the b -axis value at T_{sp} to near the a -axis value for $T > 60$ K. This feature, which is temperature dependent, becomes more prominent with increased Ni concentration. The inset of Fig. 2(b) shows that the shape of the susceptibility for a 0.8% Ni-doped crystal is nearly the same with the applied field directed along each of the three principal axes. In contrast, for higher concentrations, such as the 3.0% Ni data shown in Fig. 2(b), the c -axis susceptibility differs markedly from the other two directions. This decrease in the c -axis susceptibility suggests a change in the easy axis, from the a axis to the c axis. Measurements of the susceptibility as a function of angle between the a and c axes confirm that at 20 K, $\chi_a < \chi_c$, whereas the reverse is true at 100 K. Since the spin-Peierls transition is a lattice

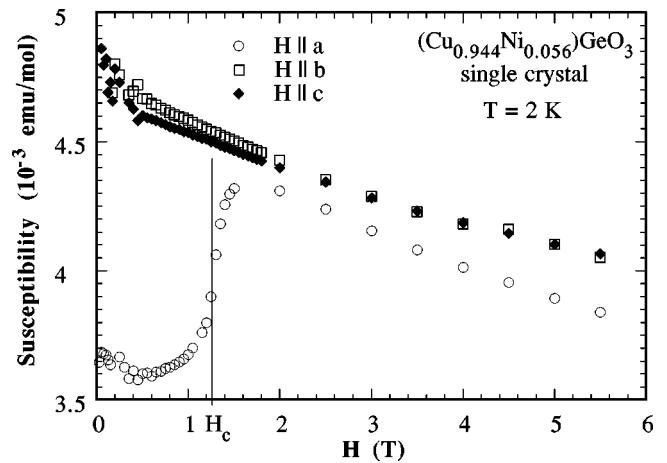


FIG. 4. The susceptibility as a function of field at $T = 2$ K for a $(\text{Cu}_{0.944}\text{Ni}_{0.056})\text{GeO}_3$ single crystal aligned with magnetic field parallel to each of the three principal axes, in turn. The spin-flop transition occurs with $H \parallel a$, at a critical field of about 1.205 T.

distortion, it is not unreasonable for the magnetic anisotropy to be different above and below T_{sp} .

As shown in Fig. 3(a), the molar susceptibility as a function of angle for a $(\text{Cu}_{0.944}\text{Ni}_{0.056})\text{GeO}_3$ single crystal confirms that the a axis is the easy axis when $H < H_c$. The susceptibility varies smoothly between the a and c axes, and the a and b axes. Similar results are found for other Ni compositions. In addition to these results at 1.8 K, measurements were made at 5 and 50 K, with similar results. Also, data for a $(\text{Cu}_{0.97}\text{Co}_{0.03})\text{GeO}_3$ single crystal are shown in the inset of Fig. 3, to highlight the different easy-axis direction for different dopants.

These measurements were repeated with an applied field of 2 T, which is well above the observed spin-flop critical field for $(\text{Cu}_{0.944}\text{Ni}_{0.056})\text{GeO}_3$ at 1.8 K. As shown in Fig. 3(b), with $H > H_c$, there is a minimum in the susceptibility at about 40° between the a and b axes, and a and c axes. A possible interpretation is as follows. With the applied field greater than the critical field, and parallel to the a axis, the spins flop away from the a axis. As the crystal is rotated, the component of the field parallel to the a axis decreases. Be-

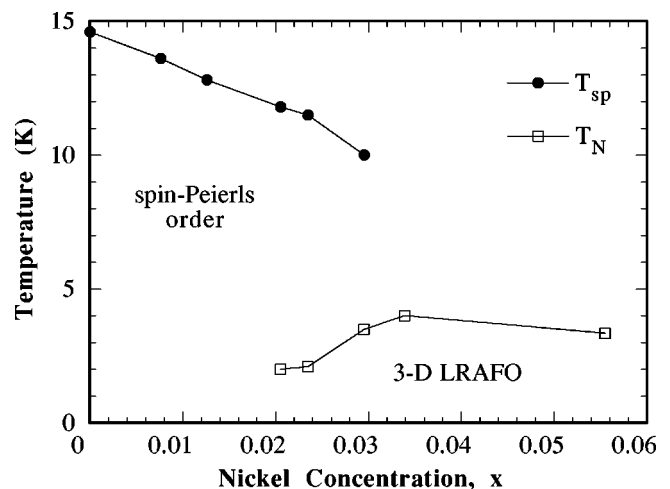


FIG. 5. The magnetic phase diagram of the $(\text{Cu}_{1-x}\text{Ni}_x)\text{GeO}_3$ system as determined by magnetic susceptibility data.

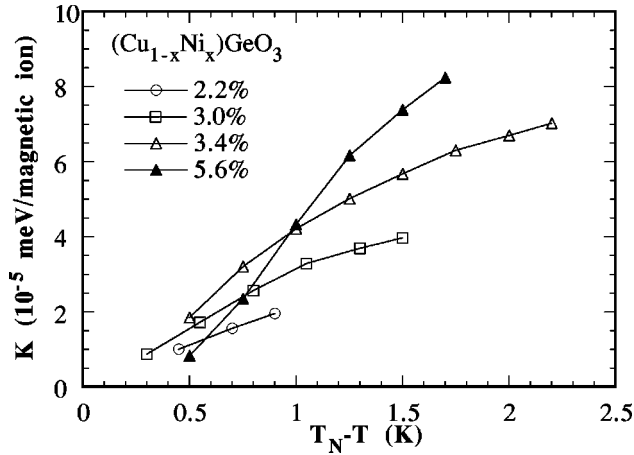


FIG. 6. The anisotropy energy as a function of the scaled temperature ($T_N - T$) for various nickel concentrations. The values were calculated, assuming uniaxial symmetry, from the measured susceptibility along the principal axes, and the measured values of the spin-flop critical field, H_c . There is one magnetic ion per formula unit for $(\text{Cu}_{1-x}\text{Ni}_x)\text{GeO}_3$.

cause the spin-flop transition is driven by a competition between the Zeeman energy and the anisotropy energy, at some point, realignment with the a axis will be energetically favorable.

It is not surprising that replacing only a few percent of the Cu ions with impurities leads to Néel order, since one-dimensional systems are relatively unstable. The fact that the easy axis changes with different impurities at low concentrations implies that single-ion anisotropy plays an important role in determining the magnetic properties of the doped CuGeO_3 system.

In order to further investigate the anisotropic nature of the $(\text{Cu}_{1-x}\text{Ni}_x)\text{GeO}_3$ system, we have made a detailed study of the spin-flop transition. With the assumption of uniaxial symmetry, the anisotropy energy (K) can be expressed as¹⁴

$$K = \frac{H_c^2(\chi_{\perp} - \chi_{\parallel})}{2}, \quad (1)$$

where H_c is the spin-flop critical field, χ_{\perp} and χ_{\parallel} are the magnetic susceptibilities perpendicular and parallel to the easy axis, respectively. For our analysis, we take H_c to be the midpoint of the transition, as determined by linear fits to the molar susceptibility data for $H \ll H_c$ and $H \gg H_c$. This point coincides with a local maximum in dM/dH . To determine $(\chi_{\perp} - \chi_{\parallel})$, the raw b -axis and c -axis susceptibilities (χ_b and χ_c) were shifted by a temperature-independent constant so that the susceptibility along all three directions coincides for $T > T_N$.

Shown in Fig. 6 is the anisotropy energy K for $x \geq 0.021$ as a function of $(T_N - T)$. The anisotropy energy increases

with increased Ni concentration. This is to be expected, since for pure CuGeO_3 , and $(\text{Cu}_{1-x}M_x)\text{GeO}_3$, with $M = \text{Zn}, \text{Co}$, and Mn , the c axis is the easy axis. Nickel impurities cause the system to order with the a axis as the easy axis, so increased nickel impurities will increase the anisotropy energy.

These values of the anisotropy energy, which we determined through measurements of the spin-flop critical field, are quite low compared with the exchange energy along the c axis in pure CuGeO_3 . Nishi *et al.*¹⁵ measured a value of $J_c = 10.4$ meV, with $J_a \approx -0.01J_c$ and $J_b \approx 0.1J_c$. Since the interchain exchange constants J_a and J_b are much smaller, it is not meaningful to compare the anisotropy energy to J_c . Using the Néel temperature as a crude estimate of the exchange coupling leading to long-range antiferromagnetic order, one would expect exchange coupling on the order of 0.26 meV ($T_N \sim 3 \text{ K} \sim 0.26 \text{ meV}$). Since anisotropy energies are generally expected to be about a factor of 10^4 smaller than the exchange energy,¹⁶ our reported values of anisotropy of Ni-doped CuGeO_3 are reasonable, especially since the measurements of H_c were done within a few Kelvin of the Néel temperature.

V. CONCLUSIONS

We have measured the magnetization of single crystals in the $(\text{Cu}_{1-x}\text{Ni}_x)\text{GeO}_3$ system as a function of temperature, magnetic field, and angle between the principal axes. The magnetic phase diagram, as determined from the susceptibility versus temperature data, agrees qualitatively with other published reports for nickel doping. With measurements of magnetization versus angle, we have confirmed that in the ordered antiferromagnetic phase, the a axis is the easy axis for nickel doping, which differs from the c axis as the easy axis observed for several other dopants: Zn, Co, Mn. We observed temperature independent, and dependent anisotropy in the susceptibility data, and suggested that the latter may be associated with a change in easy-axis direction. We have calculated the anisotropy energy from measurements of the spin-flop transition temperature, and found that the anisotropy energy increases for increased nickel doping. The unique magnetic anisotropy of the Néel phase of Ni-doped CuGeO_3 is most likely caused by the single-ion anisotropy of Ni^{+2} impurities, however, this needs to be confirmed both theoretically and experimentally.

Note added in proof. Koide *et al.* [Czech. J. Phys. **46**, (S4), 1981 (1996)] also report that the easy axis for nickel-doped CuGeO_3 is the a axis.

ACKNOWLEDGMENT

This research was supported by the National Science Foundation, under Grant No. DMR-97-01735.

¹M. Hase, I. Terasaki, and K. Uchinokura, Phys. Rev. Lett. **70**, 3651 (1993).

²H. Völlenkle, A. Wittmann, and H. Nowotny, Monatsh. Chem. **98**, 1352 (1967).

³M. Hidaka, M. Hatae, I. Yamada, M. Nishi, and J. Akimitsu, J.

Phys.: Condens. Matter **9**, 809 (1997).

⁴M. Hase, I. Terasaki, Y. Sasago, K. Uchinokura, and H. Obara, Phys. Rev. Lett. **71**, 4059 (1993).

⁵M. Hase, Y. Sasago, K. Uchinokura, G. Kido, and T. Hamamoto, J. Magn. Magn. Mater. **140**, 1691 (1995).

- ⁶S. B. Oseroff, S. W. Cheong, B. Aktas, M. F. Hundley, Z. Fisk, and L. W. Rupp, *Phys. Rev. Lett.* **74**, 1450 (1995).
- ⁷P. E. Anderson, J. Z. Liu, and R. N. Shelton, *Phys. Rev. B* **56**, 11 014 (1997).
- ⁸P. E. Anderson, J. Z. Liu, and R. N. Shelton, (unpublished) magnetization data for $(\text{Cu}_{1-x}\text{Mn}_x)\text{GeO}_3$ single crystals.
- ⁹M. Weiden, W. Richter, R. Hauptmann, C. Geibel, and F. Steglich, *Physica B* **233**, 153 (1997).
- ¹⁰Y. Sasago, N. Koide, K. Uchinokura, M. C. Martin, M. Hase, K. Hirota, and G. Shirane, *Phys. Rev. B* **54**, R6835 (1996).
- ¹¹The measurements were made with a Cameca SX-50 electron microprobe. The parameters for the electron microprobe measurements were as follows: accelerating potential=20 keV, beam current=10 nA, rastered beam at 100 000 times magnification ($\sim 1 \mu\text{m}$ square beam size,) scanning for $K\alpha$ lines of Cu, Ni, and Ge, with ZAF fluorescence absorption atomic number matrix corrections.
- ¹²Quantum Design Inc., 11578 Sorrento Valley Road, San Diego, CA 92121.
- ¹³J. G. Lussier, S. M. Coad, D. F. McMorrow, and D. M. Paul, *J. Phys.: Condens. Matter* **7**, L325 (1995).
- ¹⁴S. Chikazumi, *Physics of Magnetism* (Wiley, New York, 1964), p. 135.
- ¹⁵M. Nishi, O. Fujita, and J. Akimitsu, *Phys. Rev. B* **50**, 6508 (1994).
- ¹⁶R. J. Weiss, *Physics of Materials* (Hemisphere, New York, 1990).